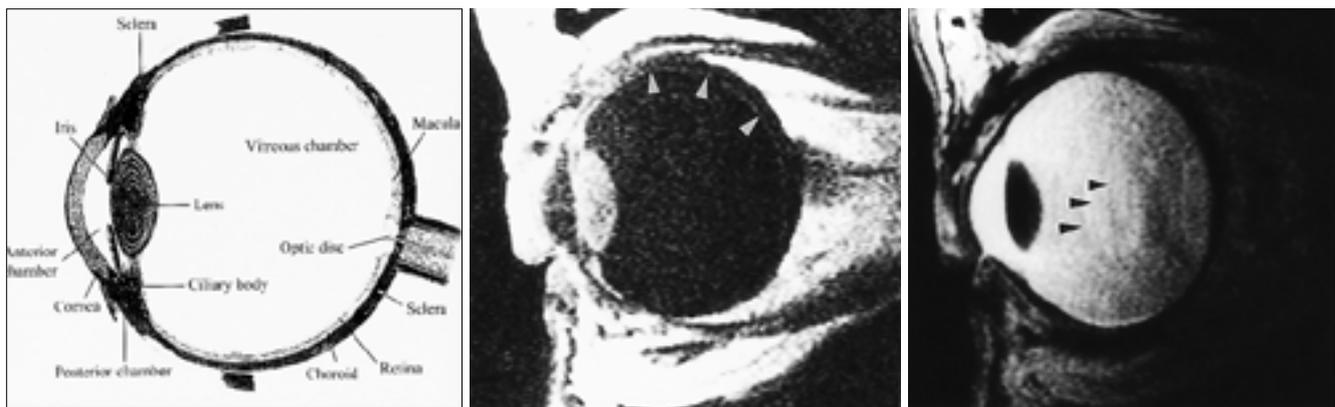
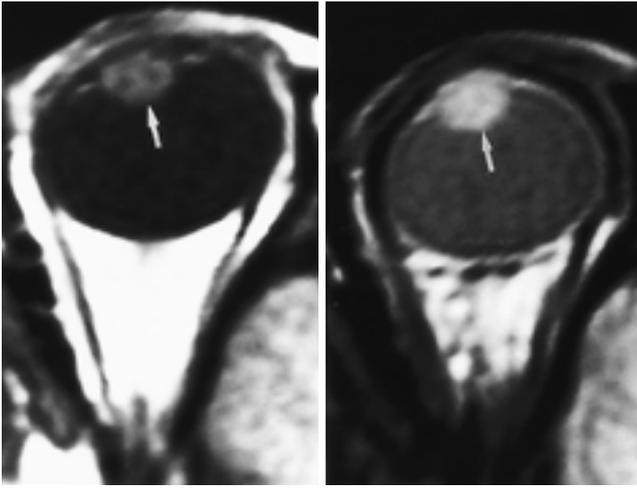




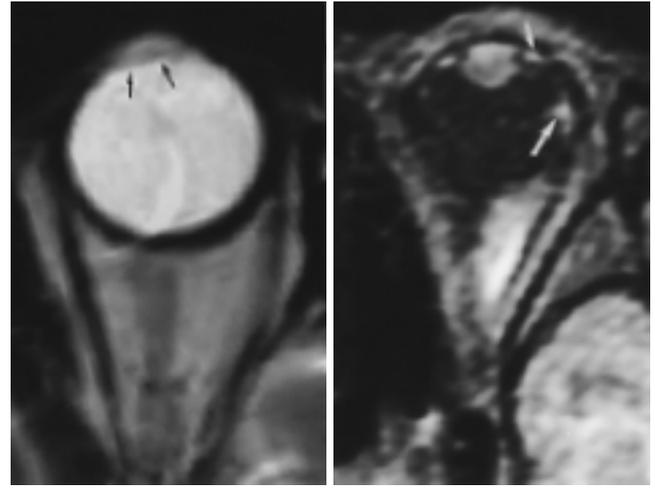
가 (7), MR (retinoblastoma) (4) (Fig. 5, 9A,B). (anophthalmos) (buphthalmos) (macrophthalmos) (Sturge-Weber type 1) (neurofibromatosis type 1) (pseudoproptosis), (lid retraction) (exophthalmos) (3). MR (Fig. 2A,B). (Deformed lens) (coloboma of the lens) (spherophakia) (microphakia), (lenticonus) (3). (secondary open angle glaucoma) (phacolytic glaucoma), (phacomorphic glaucoma), (lens induced uveitis) (3). MR (4) (Fig. 3). (Uveitis) (iritis), (cyclitis), (choroiditis) (toxoplasmosis), Behcet (Behcet's disease), (3). MR T2- (4,5) (Fig. 4). (Vitreous body) (Microphthalmos, anophthalmos and buphthalmos) (microphthalmos) (coloboma), (Vitreous hemorrhage) (4) (Fig. 6). MR (4). T1, T2 (Fig. 7A,B) (Persistent hyperplastic primary vitreous:PHPV) (hyaloic vascular system) (hyaloid artery) (leukocoria) (MR T1, T2 (4,8). (sub-retinal fluid collection)가



**Fig. 1. Normal MR anatomy of the eyeball.**  
**A.** Schematic drawing of eyeball explains anatomic subunits compared with continuing MR images. Ocular MR imaging using a 3inch surface coil shows details of the eyeball.  
**B.** T1WI differentiates the inner layers of the wall of the globe. Choroidal layer (arrowheads) is seen as linear high signal. Lens and ciliated body represent high signal intensity that is caused by field inhomogeneity (i.e. magnified signal intensity close to the coil).  
**C.** On T2WI , biconvex lens is well seen. Motion artifact is seen (arrowheads)



A B  
 Fig.2.A 3-year-old boy with congenital cataract.  
 A. T1WI shows a slightly hyperintense global lens(arrow).  
 B. Proton density weighted image shows higher signal intensity of lens(arrow) with globular shape.



3 4  
 Fig.3. A 62-year-old man with intraocular lens implantation.  
 On T2WI, the innate lens was replaced with flat artificial lens of low signal intensity(arrow).  
 Fig.4.A 40-year-old man with chronic uveitis.  
 On contrast enhanced T1WI with fat suppression, the linear enhancement in the anterior chamber suggests anterior synechia (small arrow). Another nodular enhancement along inner wall of eyeball(choroid) suggests granulation tissue(large arrow). Additionally, MR scan shows microphthalmos.

(Fig. 8).

Coats

가 . 90%  
 (4-8 )  
 T1,T2  
 가 T1,T2 V-  
 (4).  
 (Retrolental fibroplasia or retinopathy of pre-maturity)  
 가  
 (active phase), (regressive phase),  
 (cicatrical phase) 3 . MR  
 가 ,  
 가 (persistent hyperplasia primary vitreous),  
 (retinoblastoma), (endophthalmitis)  
 ( Incontinentia pigmenti)  
 X-  
 (Fig. 9 A,B).  
 (6).

(Ocular wall)  
 (Choroidal detachment)  
 Bruch  
 (serous or exudative choroidal detachment),  
 (hemorrhagic choroidal detachment)  
 (3).  
 T1 , T2  
 (4)(Fig. 10A,B).  
 가  
 (Retinal detachment )  
 (retinal pigment epithelium)  
 (neurosensory retina) 가  
 (rhegematogenous retinal detachment),  
 (tractional retinal detachment),  
 (combined tractional and rhegematogenous),  
 (hemorrhagic or serous detachment) 47가 가 가  
 가 . MR  
 (optic disc) V-  
 T1 , T2  
 (Fig. 11A,B).  
 MR T1,T2

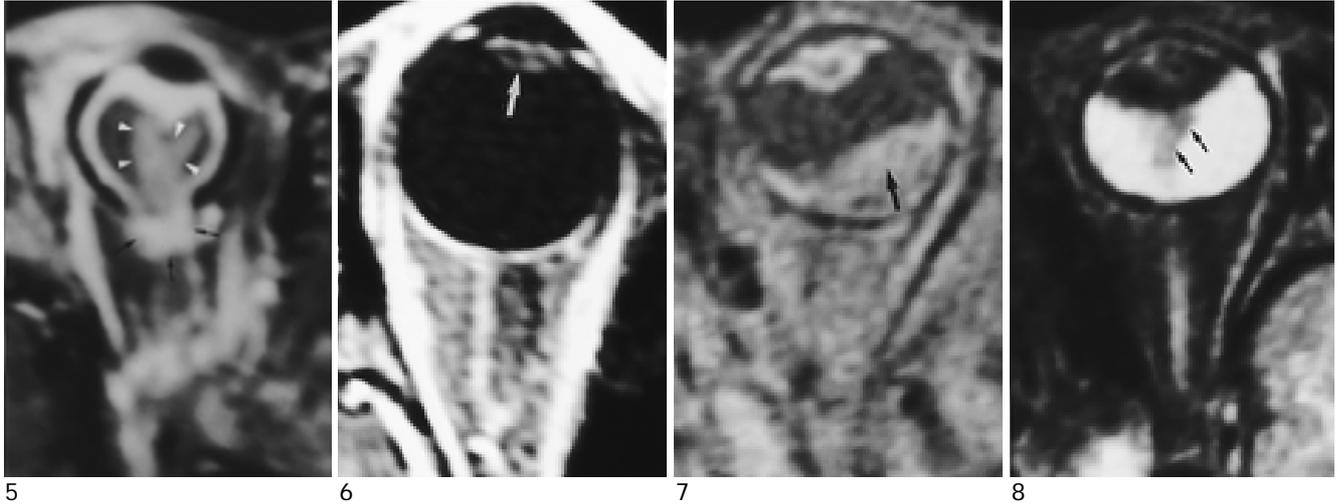


Fig. 5. A 3-year-old girl with persistent hyperplastic primary vitreous and coloboma.

Contrast enhanced T1WI with fat suppression shows microphthalmos and posterior global defect (arrows). Triangular increased signal in vitreous may suggest the persistence of fetal tissue in Cloquet's canal (arrowheads).

Fig. 6. A 48-year-old man with glaucoma and cataract.

T1WI with fat suppression shows slightly increased signal intensity of lens (arrow) and buphthalmos. Increased size of globe represents increased intraocular pressure.

Fig. 7. An infant with subhyaloid hemorrhage.

T1WI with fat suppression shows increased signal intensity (arrow) in the vitreous chamber along the ocular wall. This hyperintense fluid is thought as subhyaloid hemorrhage.

Fig. 8. A 5-year-old boy with persistent hyperplastic primary vitreous.

T1WI with fat suppression shows S-shaped linear hypointensity (arrows) of fibrovascular retrolental mass. The intravitreal tubular intensity is compatible with a remnant of primary vitreous along the hyaloid canal. Hyperintensity in vitreous suggests hemorrhage either in the subretinal space or subhyaloid space in the absence of retinal detachment.

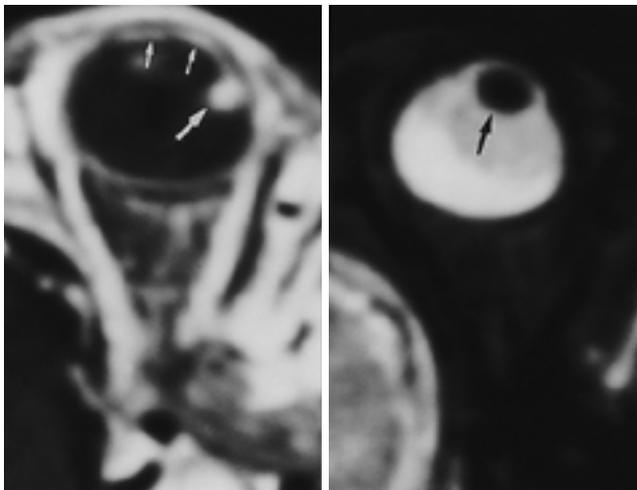


Fig. 9. An infant with incontinentia pigmenti.

A. Contrast enhanced T1WI with fat suppression shows linear enhancement of the cornea (small arrows) and nodular enhancement of the ciliary body (large arrow) suggesting anterior synechia.

B. T2WI shows a globular lens (arrow). This patient has bilateral microphthalmos, which occurs in the neonate.

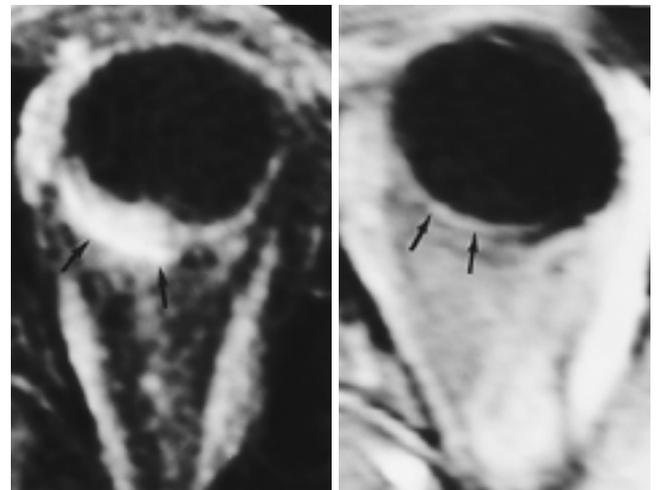


Fig. 10. A 35-year-old woman with choroidal detachment with hemorrhage.

A. Contrast enhanced axial T1WI with fat suppression. The lesion (posterior pole) shows unenhanced crescent hyperintense signal (arrows) along the ocular wall. The associated high signal intensity surrounding the globe means artifact and subretinal hemorrhage.

B. After 3 months, the choroidal hemorrhage subsided (arrows).

(4). (Coloboma of the optic disc) (fetal cleft) (leukokoria) (9) (optic disc) (4)(Fig. 5). (Retinoblastoma) 가 1/20,000 Coats , PHPV, (4). CT T1 MR T2 가 (4). (Malignant melanoma) (가 1가 , 15mm (epitheloid) (4). MR T1 T2 (24) (amelanotic melanoma)

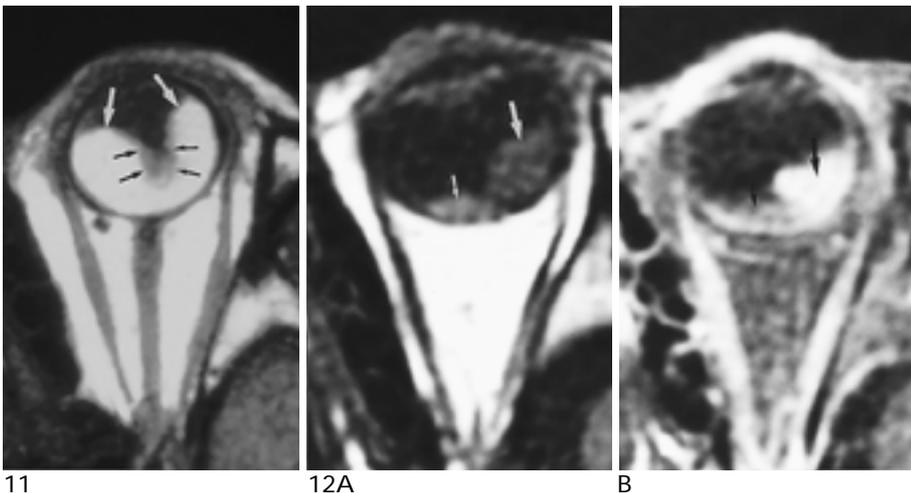


Fig.11. A boy with retinal detachment and subretinal hemorrhage. T1WI shows high signal intensity of subretinal hemorrhage(white arrows). The retina cannot be detached from the optic disc. Characteristic folding of retinal leaves(black arrows) toward to optic disc is seen.

Fig. 12. A 2-year-old girl with retinoblastoma. A. T1WI shows a slightly hyperintense mass(large arrow) and retinal hemorrhage (small arrow). The differentiation of a mass and associated retinal hemorrhage is difficult. B. Contrast enhanced T1WI with fat suppression shows a strong enhancement of retinoblastoma that has strong enhancement(large arrow) compared to the high signal intensity of the surrounding hemorrhage(small arrow).

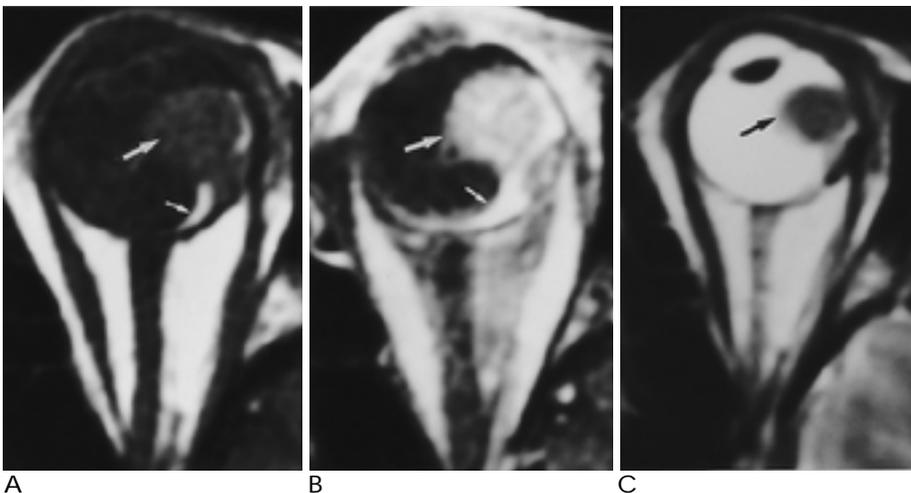
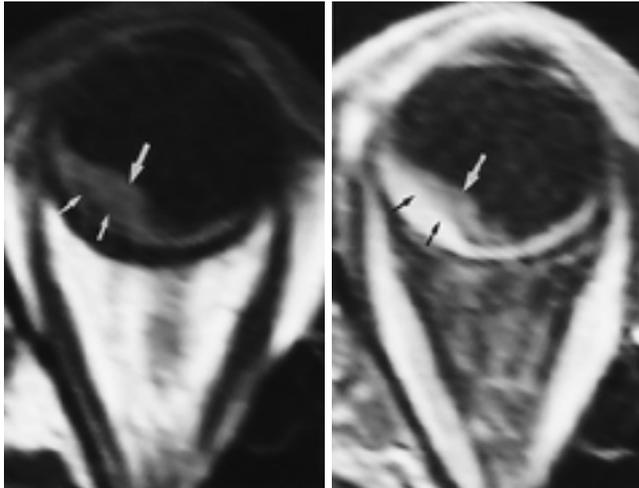


Fig. 13. A 39-year-old woman with primary malignant melanoma. A. T1WI shows mushroom morphology of the choroidal melanoma(large arrow). This tumor is proved as amelanotic melanoma. Subretinal hemorrhage(small arrow) is associated. B. Contrast enhanced T1WI with fat suppression shows strong enhancement of tumor(large arrow) compared to high signal intensity of retinal hemorrhage(small arrow). C. T2WI shows a hypointense tumor (arrow).



A B  
 Fig. 14 A 53-year-old man with choroidal metastasis from lung cancer.  
 A. T1WI shows a crescentic slight hypointense mass (small arrows) with choroidal hemorrhage (large arrow).  
 B. Contrast enhanced T1WI with fat suppression shows strong enhancement of a choroidal mass (small arrows) compared to nonenhanced choroidal hemorrhage (large arrow).

T1

(Fig. 13A,B,C)

(Choroidal metastasis)

10%

1/3

(neuroblastoma), Ewing Wilms

가 (2,9).

MR

가

(Fig. 14A,B).

1. Clemente CD. *Organs of the special senses. Gray's Anatomy*. 30th ed. Philadelphia : Lea and Febiger, 1985 : 1290-1303
2. Valvassori GE, Mafee MF, Carter BL. *Imaging of the head and neck*. New York : Thieme, 1995 : 157-245
3. , 1994 : 129-152
4. Potter PD, Shields JA, Shields CL. *MRI of the eye and orbit*. Philadelphia : B.Lippincott Company, 1995 : 31-34, 55-62, 93-98
5. Hardjasudarma M, Ganley JP, McClellan RL et al. Non neoplastic chorioretinal enhancement patterns in magnetic resonance imaging of the eye. *Cannad Assoc Radiol J* 1995 ; 46 : 183-188
6. Wolpert SM, Barness PD. *MRI in pediatric neurology*. St. Louis : Mosby Year Book, 1992 : 326
7. Vaughan DG, Asburg Taylor, Paul Riordan-Eva. *General ophthalmology*. 13th ed. Norwalk : Appleton and Lange, 1992 : 169 212
8. CT MR , 1994 ; 30 : 1141-1146
9. Som PM, Bergerson RT. *Head and neck imaging*. 3rd ed. St. Louis : Mosby Year Book, 1996 : 1009 1059

J Korean Radiol Soc 1999;40:1071-1076

## MR Imaging of the Eyeball : Anatomy and Pathology<sup>1</sup>

Dong Hun Kim, M.D., Ho Kyu Lee, M.D., Young Hee Yoon, M.D.<sup>2</sup>,  
 Choong Gon Choi, M.D., Dae Chul Suh, M.D.

<sup>1</sup>Department of Diagnostic Radiology, Asan Medical Center, University of Ulsan, College of Medicine

<sup>2</sup>Department of Ophthalmology, Asan Medical Center, University of Ulsan, College of Medicine

The eyeball can be divided into the anterior and posterior compartment bordering on the lens. The ocular wall is composed of three layers, namely the sclera, choroid and retina. Different pathologic conditions can occur, depending on the anatomic location. This paper illustrates the anatomical features of normal eyeball, as seen on MRI, and a variety of pathologic conditions of the compartments. An understanding of the MR features of various intraocular lesions is thus facilitated.

**Index words :** Eye, MR  
 Orbit, neoplasms

Address reprint requests to : Ho Kyu Lee, M.D., Department of Diagnostic Radiology, Asan Medical Center College of Medicine University of Ulsan  
 #388-1 Poongnap-dong, Song pa-Gu, Seoul 138-736, Korea.  
 Tel. 82-2-2224-4371 Fax. 82-2-476-4719